

Comparative Simulation Study of Three Control Techniques Applied to a Biped Robot

Mark Raibert*, Spyros Tzafestas**, Costas Tzafestas**

* AI Lab., MIT, 545 Tech. Square
Cambridge, Mass 02139, USA

** IRCU, National Tech. Univ. of Athens
Zografou, 15773 Athens, GREECE

Abstract This paper provides a comparative study, through simulation, of the effectiveness of the local (decoupled) PD control, the computed torque control, and the sliding mode robust control when applied to a 5-link biped robot model. The superiority of the sliding mode control in case of existence of large parametric uncertainty is verified. It is argued that sliding mode control appropriately smoothed can be used successfully in actual (experimental or not) bipeds to increase their performance capabilities.

I. INTRODUCTION

The mechanical complexity of legged locomotion systems is one of the characteristics that make their study and design very difficult. In particular, the existence of a non (directly) controllable degree of freedom in biped systems plays a dominant role in the determination and improvement of their stability properties. On the other hand, during the motion of any walking robot, a number of sudden geometric constraints are imposed, e.g. stepping on the ground, knee locking, etc. These constraints, which are inherent in all walking machines, give rise to impulse-like disturbances that make the control by standard PD or PID controllers an extremely difficult problem.

The analysis, design and construction of anthropomorphic bipeds has received in recent years a particular attention and currently, many biped robot prototypes exist in academic and other institutions [1-7]. In the present paper the effectiveness of robust sliding mode control applied to a 5-link biped robot is studied and compared to that of the usual computed torque and decoupled PD control. The theoretical expectation that sliding mode control is much superior than local PD control and computed torque control in the presence of strong parametric uncertainty is fully verified. The fact that this superiority is strengthened as the uncertainty level of the biped model increases is also established. Through the selection of appropriate reference signals a stable walk of the biped, both on an horizontal plane surface and on a staircase, is achieved. It is observed that if the uncertainty level is very high (higher than 80%) it may not be possible to maintain a stable gait with usual PID

control. The computational complexity of both the computed torque and the sliding mode control allow their realization with standard microprocessor hardware and software. In particular, if the algorithms are programmed in *assembly*, the computation time is of the order of 3-4 msec. Further, by using suitable fast inverse dynamics algorithms (such as the Luh-Walker-Paul algorithm, [8]) or by parallelizing the computations, this figure can go down to less than 1-2 msec. Another improvement can be obtained if all the trigonometric functions are prestored and called from a ROM memory. Thus, since a sampling frequency of at least 60 Hz ($T_s \leq 16\text{msec}$) leads to a very good trajectory tracking performance, it can be argued that the sliding mode control is suitable for use in experimental and practical biped robotic systems.

II. THE BIPED DYNAMIC ROBOTIC MODEL

The biped robot model of the present study has five links (torso and two links in each leg) and has the form of Fig. 1.

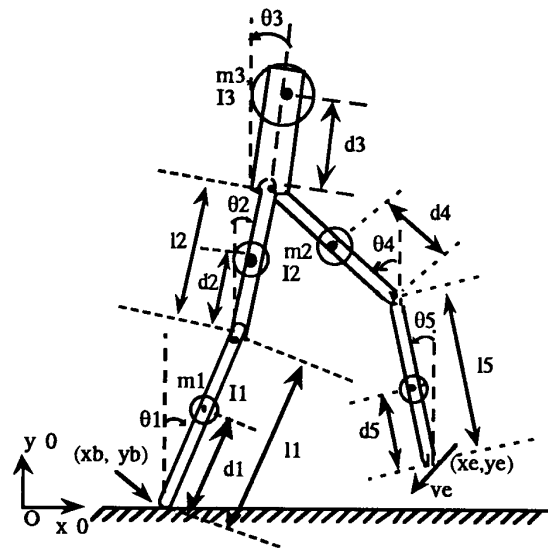


Fig. 1. 5-link planar biped robot model

These links are connected via four rotating joints (two hip and two knee joints) which are assumed to be friction free, and each one of them is driven by an independent dc motor. The locomotion takes place on the sagittal plane as shown in Fig.1. Since this biped does not have ankle joints and feet, variation of its speed through torques at these joints is not possible. The biped, however, can walk indirectly using the effect of gravity.

From Fig.1 it follows that

$$x_e = x_b + l_1 \sin \theta_1 + l_2 \sin \theta_2 + l_4 \sin \theta_4 + l_5 \sin \theta_5 \quad (1a)$$

$$y_e = y_b + l_1 \cos \theta_1 + l_2 \cos \theta_2 - l_4 \cos \theta_4 - l_5 \cos \theta_5 \quad (1b)$$

and

$$v_e = \begin{pmatrix} \dot{x}_e \\ \dot{y}_e \end{pmatrix} = \begin{pmatrix} l_1 \cos \theta_1 \\ -l_1 \sin \theta_1 \end{pmatrix} \dot{\theta}_1 + \begin{pmatrix} l_2 \cos \theta_2 \\ -l_2 \sin \theta_2 \end{pmatrix} \dot{\theta}_2 + \begin{pmatrix} l_4 \cos \theta_4 \\ l_4 \sin \theta_4 \end{pmatrix} \dot{\theta}_4 + \begin{pmatrix} l_5 \cos \theta_5 \\ l_5 \sin \theta_5 \end{pmatrix} \dot{\theta}_5 \quad (2)$$

Now, if (c_gx, c_gy) are the coordinates of the biped's center of mass, and (x_{ci}, y_{ci}) the coordinates of the center of mass of link i then

$$\left. \begin{aligned} x_{c1} &= d_1 \sin \theta_1, & y_{c1} &= d_1 \cos \theta_1 \\ x_{c2} &= l_1 \sin \theta_1 + d_2 \sin \theta_2, & y_{c2} &= l_1 \cos \theta_1 + d_2 \cos \theta_2 \\ x_{c3} &= l_1 \sin \theta_1 + l_2 \sin \theta_2 + d_3 \sin \theta_3 \\ y_{c3} &= l_1 \cos \theta_1 + l_2 \cos \theta_2 + d_3 \cos \theta_3 \\ x_{c4} &= l_1 \sin \theta_1 + l_2 \sin \theta_2 + (l_4 - d_4) \sin \theta_4 \\ y_{c4} &= l_1 \cos \theta_1 + l_2 \cos \theta_2 - (l_4 - d_4) \cos \theta_4 \\ x_{c5} &= l_1 \sin \theta_1 + l_2 \sin \theta_2 + l_4 \sin \theta_4 + (l_5 - d_5) \sin \theta_5 \\ y_{c5} &= l_1 \cos \theta_1 + l_2 \cos \theta_2 - l_4 \cos \theta_4 - (l_5 - d_5) \cos \theta_5 \end{aligned} \right\} (3)$$

and

$$\left. \begin{aligned} c_gx &= \frac{(m_1 x_{c1} + m_2 x_{c2} + m_3 x_{c3} + m_4 x_{c4} + m_5 x_{c5})}{(m_1 + m_2 + m_3 + m_4 + m_5)} \\ c_gy &= \frac{(m_1 y_{c1} + m_2 y_{c2} + m_3 y_{c3} + m_4 y_{c4} + m_5 y_{c5})}{(m_1 + m_2 + m_3 + m_4 + m_5)} \end{aligned} \right\} (4)$$

A. Single-Leg-Support Phase

This situation is schematically shown in Fig.2. It is assumed that the friction of the ground is sufficiently large to ensure no slipping of the supporting end. Since the motion of the biped is performed on the plane of Fig.1 the angles θ_i ($i=1,2,\dots,5$) are sufficient for fully describing its configuration.

The Lagrange dynamic model describing the motion of the biped in this phase is found to be :

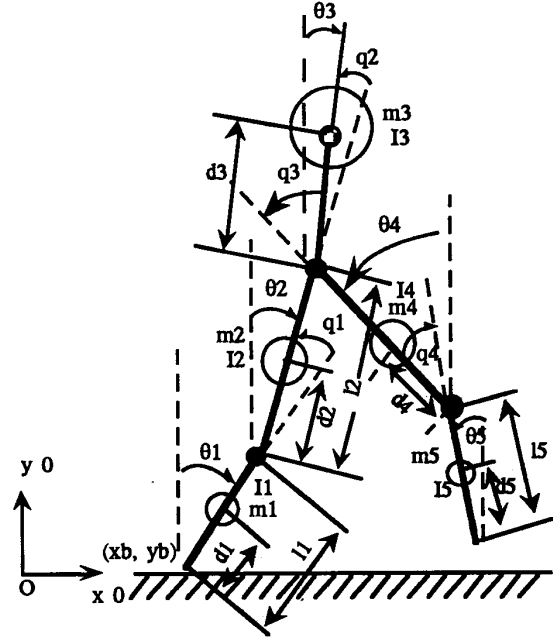


Fig. 2. Biped with one leg in the air

$$D(\theta) \cdot \ddot{\theta} + h(\theta, \dot{\theta}) + G(\theta) = T_\theta \quad (5)$$

where

$$\theta = [\theta_1, \theta_2, \dots, \theta_5]^T, \quad T_\theta = [T_{\theta_1}, \dots, T_{\theta_5}]^T$$

$$h(\theta, \dot{\theta}) = \text{col} \left[\sum_{j=1(j \neq i)}^5 \left(h_{ijj} (\dot{\theta}_j)^2 \right) \right] \quad (6)$$

$$G(\theta) = \text{col} [G_i(\theta)], \quad D(\theta) = [D_{ij}(\theta)], \quad (i,j=1,2,\dots,5)$$

Here T_{θ_i} is the generalized torque that corresponds to θ_i , $\text{col}[a_i]$ is a column vector with elements a_i , and $D(\theta)$ is the inertia matrix of the biped.

Now, let $\tau = [\tau_1, \tau_2, \tau_3, \tau_4]^T$ be the vector of the driving torques of the four joints of the biped, where (Fig.2):

- τ_1 : driving torque of the knee of the supporting leg
- τ_2 : driving torque of the hip of the supporting leg
- τ_3 : driving torque of the hip of the free leg
- τ_4 : driving torque of the knee of the free leg

If q_1, q_2, q_3 and q_4 are the relative angle deflections of the corresponding joints, then (see Fig.2):

$$q_1 = \theta_1 - \theta_2, \quad q_2 = \theta_2 - \theta_3, \quad q_3 = \theta_3 + \theta_4, \quad q_4 = \theta_4 - \theta_5$$

and so the relation

$$T_{\theta_i} = \sum_{j=1}^4 \tau_j \frac{\partial q_j}{\partial \theta_i}, \quad i = 1, 2, \dots, 5$$

gives

$$T_{\theta} = E \cdot \tau$$

where E is the 5x4 matrix

$$E = \begin{bmatrix} 1 & 0 & 0 & 0 \\ -1 & 1 & 0 & 0 \\ 0 & -1 & 1 & 0 \\ 0 & 0 & 1 & 1 \\ 0 & 0 & 0 & -1 \end{bmatrix}$$

Thus the biped dynamic model (5) becomes

$$D(\theta) \cdot \ddot{\theta} + h(\theta, \dot{\theta}) + G(\theta) = E \cdot \tau \quad (7)$$

One observes that only four of the five degrees of freedom $\theta_1, \theta_2, \dots, \theta_5$ can be controlled directly by the four driving torques τ_1, τ_2, τ_3 and τ_4 . The angle θ_1 at the contact point with the ground (hypothetical joint 0) is controlled only indirectly using the gravitational effect.

To facilitate the control procedure, to be described in Section III, the model (7) is transformed to :

$$D_q(q) \cdot \ddot{q} + h_q + G_q = T_q \quad (8a)$$

where (here $T_{q_0}=0$) $q = \text{col}[q_j]$, $h_q = \text{col}[h_{qj}]$,

and $G_q = \text{col}[G_{qj}]$, $T_q = \text{col}[T_{qj}]$ ($j = 0 \dots 4$)

$$\left. \begin{aligned} D_q(i, 1) &= A_{i1} + A_{i2} + A_{i3} - A_{i4} - A_{i5} \\ D_q(i, 2) &= -A_{i2} - A_{i3} + A_{i4} + A_{i5} \\ D_q(i, 3) &= -A_{i3} + A_{i4} + A_{i5} \\ D_q(i, 4) &= A_{i4} + A_{i5} \\ D_q(i, 5) &= -A_{i5} \end{aligned} \right\} \quad (8b)$$

This model uses the variables q_i ($i = 0, 1, \dots, 4$) instead of θ_i ($i = 1, 2, \dots, 5$), where q_0 corresponds to the hypothetical joint 0 at the contact point (x_b, y_b) with $q_0 = \theta_1$. Due to space limitations, the expressions for the A_{ij} 's are omitted here (see [12]).

B. Biped-in-the-Air Phase

Suppose now that at the moment when the free leg touches the ground, the supporting leg leaves the ground, so that the biped is actually in the air. This means that at the moment of collision of the free end with the ground the constraint $x_b = y_b = \text{constant}$ and $\dot{x}_b = \dot{y}_b = 0$, which was valid in the single-leg-support phase, is removed (see Fig. 2). This implies that the dynamic model (5) or (8a) of the

single-leg-support phase cannot be applied to compute the instantaneous changes of the joint angular velocities at the moment when the free end of the biped collides with the ground.

Our purpose here is to present the biped dynamic equations when both legs are in the air. In this case, for a full description of the configuration and the position of the biped, one needs, in addition to θ_i ($i=1,2,\dots,5$) the coordinates x_b and y_b of the left end of the biped.

Applying the standard procedure through the Lagrange equations one finds the following dynamic model for the biped in the air :

$$D_a(\theta_a) \cdot \ddot{\theta}_a + h_a(\theta_a, \dot{\theta}_a) + G_a(\theta_a) = T_a \quad (9)$$

where $\theta_a = [\theta_1, \dots, \theta_5, x_b, y_b]^T$

$$G_a = [G_a(1), \dots, G_a(7)]^T,$$

$$G_a(i) = G_i, \quad (i=1, \dots, 5), \quad G_a(6) = 0 \quad \text{and} \quad (10)$$

$$G_a(7) = \left(\sum_{i=1}^5 m_i \right) g = m_{o\lambda} \times g$$

For the 7x1 vectors T_a and h_a we have

$$T_a(i) = T_{\theta}(i), \quad i=1, \dots, 5$$

$$T_a(6) = T_{x_b} = 0, \quad T_a(7) = T_{y_b} = 0.$$

$$h_a(i) = h(i), \quad i = 1, \dots, 5$$

$$\begin{aligned} h_a(6) &= -p_{16}(\dot{\theta}_1)^2 \sin \theta_1 - p_{26}(\dot{\theta}_2)^2 \sin \theta_2 \\ &\quad - p_{36}(\dot{\theta}_3)^2 \sin \theta_3 - p_{46}(\dot{\theta}_4)^2 \sin \theta_4 \\ &\quad - p_{56}(\dot{\theta}_5)^2 \sin \theta_5 \end{aligned}$$

$$\begin{aligned} h_a(7) &= -p_{17}(\dot{\theta}_1)^2 \cos \theta_1 - p_{27}(\dot{\theta}_2)^2 \cos \theta_2 \\ &\quad - p_{37}(\dot{\theta}_3)^2 \cos \theta_3 + p_{47}(\dot{\theta}_4)^2 \cos \theta_4 \\ &\quad + p_{57}(\dot{\theta}_5)^2 \cos \theta_5 \end{aligned}$$

C. Impact of the free end on the ground.

As said before when the free end of the biped, at the completion of each step, comes into contact with the ground, then an instantaneous exchange of the support of the biped to this end is taking place, while the other end (i.e. the previous supporting leg) leaves immediately the ground. This process is assumed to take place in an infinitesimal time interval, equal to the duration of the impact of the free end with the ground. The instantaneous change $\Delta \dot{\theta}$ of the angular velocities $\dot{\theta}_i$, $i=1,2,\dots,5$, of the links, at the moment of the collision of the free end with the ground, is given by [9] :

$$\Delta \dot{\theta} = D_a^{-1} \cdot J_a^T \cdot (J_a \cdot D_a^{-1} \cdot J_a^T)^{-1} \cdot \Delta \dot{x}_e \quad (11)$$

The new angular velocities of the links, after the exchange of the supporting leg, are used as initial conditions for the new step. In this way one can simulate and study the continuous locomotion of the biped.

The 2x7 Jacobian matrix J_a of the biped in the air is given by

$$J_a = \frac{\partial x_e}{\partial \theta_a} \quad (\text{matrix : } 2 \times 7)$$

where the position vector $x_e = [x_e, y_e]^T$ is given by (1) and θ_a is the vector defined in (10).

Given that the velocity v_e becomes zero immediately after the collision with the ground, we have

$$\Delta \dot{x}_e = -\dot{x}_{e, \text{before}}$$

where $\dot{x}_{e, \text{before}}$ is the velocity of the free end just before its contact with the ground. Therefore, the formula (11) gives

$$\dot{\theta}_{\text{after}} = \dot{\theta}_{\text{before}} + D_a^{-1} \cdot J_a^T \cdot (J_a \cdot D_a^{-1} \cdot J_a^T)^{-1} \cdot (-\dot{x}_{e, \text{before}}) \quad (12)$$

where $\dot{\theta}_{\text{before}}$ and $\dot{\theta}_{\text{after}}$ are the link velocities just before and just after the exchange of the supporting leg respectively.

III. REVIEW OF THE THREE CONTROL TECHNIQUES

The dynamic performance of the biped is described by the model (8a) in the single-leg support phase, and by the model (9) when both legs are in the air. These models have exactly the same form, which for convenience is rewritten here as

$$D(q) \cdot \ddot{q} + h(q, \dot{q}) = \tau \quad (13)$$

where τ is the vector of the driving forces and here the term $h(q, \dot{q})$ involves all terms due to centripetal, Coriolis and gravitational forces. This term is strongly nonlinear and its effect increases drastically as the velocities of the biped's joints increase. Any linear control law ignores totally these nonlinearities. The approach of linearizing the dynamic model

(13) about some (fixed) operating point $x_0 = [q_0, \dot{q}_0 = 0]$ and applying linear control laws is based on the assumption that the system state actually remains in the closed vicinity of x_0 . If this is not true (which is the case in most practical situations) then the performance of this approach may not be acceptable.

In addition to the existence of the nonlinearities, the system involves uncertainties due to several sources, the primary of which is the uncertainty in the biped robot parameters. This parametric uncertainty requires the

introduction of suitable nonlinear terms in the control law that makes it robust.

Our aim here is to study and compare the performance of the following three techniques through simulations :

- (i) Local (decoupled) PD control
- (ii) Computed torque control
- (iii) Sliding mode control

A. Local PD Control

The local PID control law has the form

$$\tau_j = -K_{jD} \dot{q}_j - K_{jP} q_j - K_{jI} \int_0^t q_j(t') dt' \quad (14)$$

where $q_j = q_j(t) - q_{dj}(t)$, ($j = 1, 2, \dots, n$), is the tracking error and the feedback coefficients K_{jD} , K_{jP} and K_{jI} are positive.

Omitting the integral term gives the PD control law

$$\tau = -K_P \dot{q} - K_D q \quad (15)$$

where $K_P = \text{diag} [K_{jP}]$ and $K_D = \text{diag} [K_{jD}]$ are symmetric positive definite matrices. It can be shown through Lyapunov's direct method that under the assumption that there does not exist friction and gravity, the position control obtained using the PD algorithm (15) is successful.

To compensate for the effect of gravity one must add to (15) the feedforward term $\hat{g}(q)$ where $\hat{g}(q)$ is the available estimate of $g(q)$.

B. Computed Torque Control

The computed torque control is actually based on the feedback linearization technique, i.e. on the use of a control law structure similar to that of the system's dynamic model. Thus, the computed torque control law for the model (13) has the structure :

$$\tau = D(q)u + h(q, \dot{q}) \quad (16)$$

and eliminates the nonlinearities involved in the model (13). Indeed, using the control law (16) in (13), and assuming that $D(q)$ is invertible (away from the singular configurations), yields:

$$\ddot{q} = u \quad (17)$$

The model (17) represents a set of $n=5$ decoupled double integration systems, each one of which can be controlled by a suitable linear control law.

If the PD control law is used (with the extra feedforward term \ddot{q}_d the closed-loop equation obtained for the error q is

$$\ddot{q} + K_D \cdot \dot{q} + K_P \cdot q = 0 \quad (18)$$

It is easy to verify that if the matrices K_D and K_P are positive definite (i.e. if $K_{D_j} > 0$ and $K_{P_j} > 0$ for all j) then the tracking error tends to zero asymptotically. If λ is the desired bandwidth (undamped cyclic natural frequency) then, to obtain a critically damped closed-loop performance one must select

$$K_D = \text{diag} [2\lambda] \text{ and } K_P = \text{diag} [\lambda^2] \quad (19)$$

C. Sliding mode control

The basic drawback of the computed torque technique is that in practice $D(q)$ and $h(q, \dot{q})$ are not known exactly but approximately as $\hat{D}(q)$ and $\hat{h}(q, \dot{q})$. This uncertainty may be the result of parametric uncertainty or restricted computational power. In practice therefore one can only use the control law :

$$\tau = \hat{D}(q) u + \hat{h}(q, \dot{q}) \quad (20)$$

which leads to the system (instead of (17)):

$$\ddot{q} = (D^{-1} \hat{D}) u + D^{-1} (\hat{h} - h) \quad (21)$$

Thus the system is actually coupled and nonlinear, and the linear PD or PID control law may lead to unacceptable performance. To face this problem one has to robustify in some way the computed torque control law (20). Among the different robust control techniques the *sliding mode* technique [10-11] was selected here for application to our biped model.

If \hat{D} and \hat{h} are the available estimates of D and h , at each time instant t , then the sliding mode controller has the form (20) with u_i ($i=1,2,\dots,n$) being determined by

$$u_i = L_i(q) [\hat{u}_i - \bar{k}_i(q, \dot{q}) \text{sat}(s_i/\Phi_i)] \quad (22)$$

where $\bar{k}_i(q, \dot{q})$ and Φ_i ($i=1,2,\dots,n$) are defined by the so-called balancing equations and the \hat{u}_i 's are chosen as :

$$\hat{u}_i = \ddot{q}_{d_i} - 2\lambda \dot{q}_i - \lambda^2 q_i \quad (23)$$

The sliding surfaces s_i in (22) are selected as :

$$s_i = \dot{q}_i + 2\lambda q_i + \lambda^2 \int_t q_i(t') dt' \quad (24)$$

where the indefinite integral \int_t (which contains a constant to be determined) is defined so as $s_i(t=0)=0$. The gain coefficient $L_i(q)$ and the uncertainty bounds that are used for computing $\bar{k}_i(q, \dot{q})$ are appropriately selected. The details are not included here ([12]).

Clearly the main difference of the control law (22)-(23) from the simple computed torque PD control law is the presence of the *robustification term* :

$L_i(q) \cdot \bar{k}_i(q, \dot{q}) \text{sat}(s_i/\Phi_i)$ which ensures stability and best performance in spite of the uncertainty in the biped model.

IV. SIMULATION RESULTS

The 5-link biped shown in Fig.1 was used throughout the simulation study. The results were obtained for two different bipeds a small one and a human-sized one. The values of the parameters m_i , I_i , l_i and d_i for these two cases are shown in Tables 1 and 2.

TABLE 1
PARAMETERS OF THE SMALL SIZE BIPED ROBOT

| Link | mass m_i (Kg) | Moment of Inertia I_i (Kg m) | Length l_i (m) | Location of center of mass d_i (m) |
|-------|--------------------|--------------------------------------|---------------------|--|
| Torso | 14.79 | 3.30×10^{-2} | 0.486 | 0.282 |
| Thigh | 5.28 | 3.30×10^{-2} | 0.302 | 0.236 |
| Leg | 2.23 | 3.30×10^{-2} | 0.332 | 0.189 |

TABLE 2
PARAMETERS OF THE HUMAN-SIZED BIPED ROBOT

| Link | mass m_i (Kg) | Moment of Inertia I_i (Kg m) | Length l_i (m) | Location of center of mass d_i (m) |
|-------|--------------------|--------------------------------------|---------------------|--|
| Torso | 49.00 | 2.350 | - | 0.280 |
| Thigh | 7.63 | 0.089 | 0.431 | 0.247 |
| Leg | 4.55 | 0.105 | 0.502 | 0.267 |

Our basic goal is to realize a steady stable gait on an horizontal plane. Such a gait can be obtained by feeding to the control system repeatedly at every step the same reference signal [4]. The reference signals used here for the control of joints 1,3 and 4 are shown in Fig.3. These signals were applied in all but the first (starting) step. At the starting step the slightly different reference signals of Fig.4 were used.

A. Computed torque versus local PD control

The computed torque control law has the form (see (16) and (8a,b)):

$$T_q = D_q(q)u + h_q + G_q$$

where u is the 5X1 state feedback vector with components

$$u_1 = - \frac{1}{D_q[1,1]} \left\{ \sum_{j=1}^4 (D_q[1,j+1] u_{j+1}) + h_q(1) + G_q(1) \right\} \quad (25a)$$

$$u_{j+1} = \ddot{q}_{rj} - K_{Dj} \dot{e}_j - K_{Pj} e_j \quad (j = 1, 2, 3, 4) \quad (25b)$$

The constants K_{Dj} and K_{Pj} are selected as described in Section IIIB, i.e. $K_{Dj} = 2\lambda$ and $K_{Pj} = \lambda^2$ ($j=1,2,3,4$) (see (19)). In this way a critically damped system is obtained with control bandwidth λ . Thus, the only parameter that remains for selection is the parameter λ . Here we assume a maximum control bandwidth of 300 rad/sec ($\lambda \leq 300$ rad/sec) and a sampling period $T_s = 2\text{msec}$ ($f_s = 500$ Hz).

The results for $\lambda = 100$, $\lambda = 150$ and $\lambda = 200$ are summarized in Table 3 where by vanishing period we indicate the time period in which the error vanishes.

TABLE 3
COMPUTED TORQUE RESULTS

| λ rad/sec | Average error (rad) | Vanishing period (sec) |
|----------------------|------------------------|---------------------------|
| 100 | 0.0123 | 0.10 |
| 150 | 0.0070 | 0.05 |
| 200 | 0.0014 | 0.04 |

The tracking error obtained by local PD control with $\lambda = 200$, has the form shown in Fig.5. One observes here the existence of a steady state error (although very small) in contrast with the computed torque control where the error is always returned to zero in a given finite time. The corresponding average tracking error is now 0.0107 rads. The superiority of computed torque PD control over local PD control is strengthened if we have the human-sized biped. The results of the local PD control are shown in Figs. 6 and 7 showing an average tracking error 0.0359 rads over a period of 3 sec.

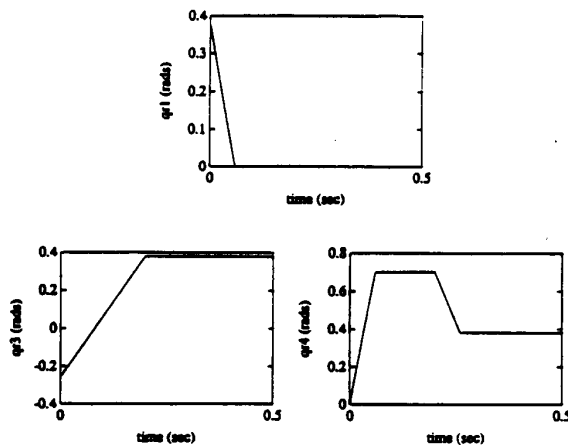


Fig.3. Reference signals for steady walking on an horizontal surface

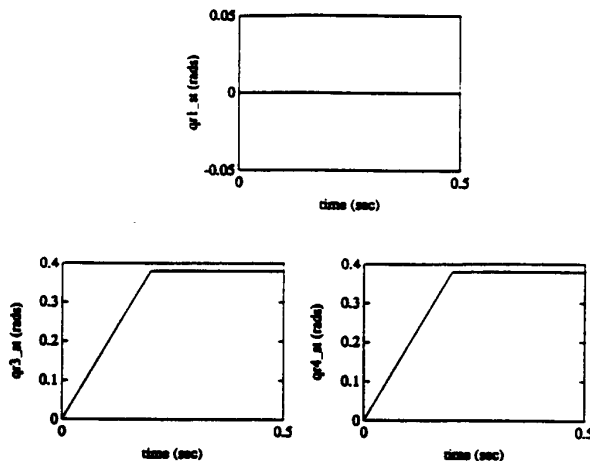


Fig.4. Reference signals for the starting step (from the vertical position).

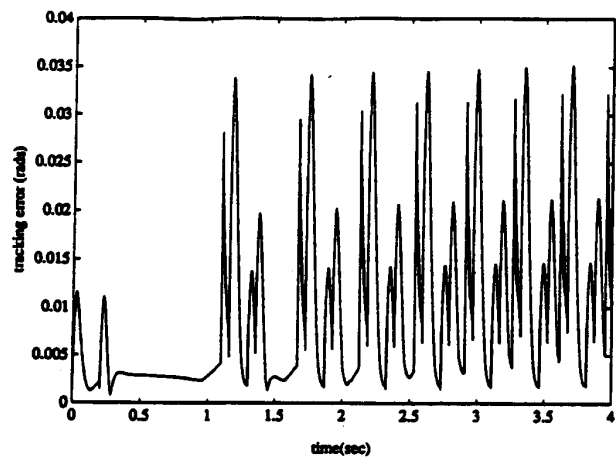


Fig.5. Tracking error of local PD control for $\lambda=200$.

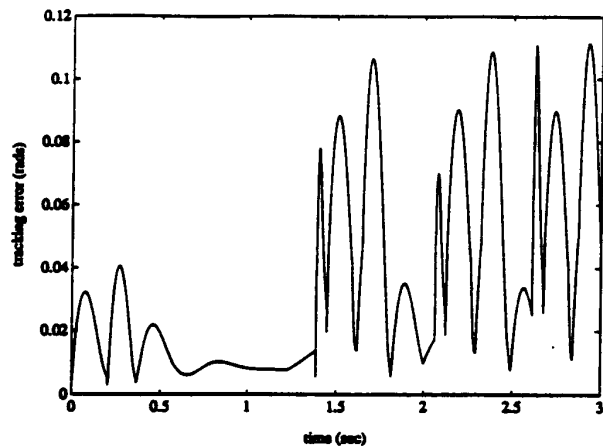


Fig.6. Tracking error of the human-sized biped for local PD control.

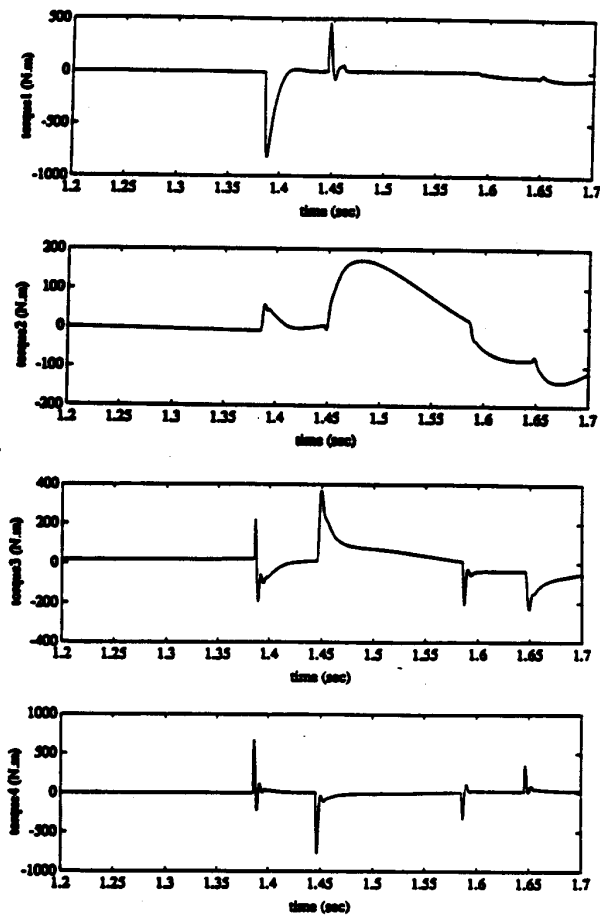
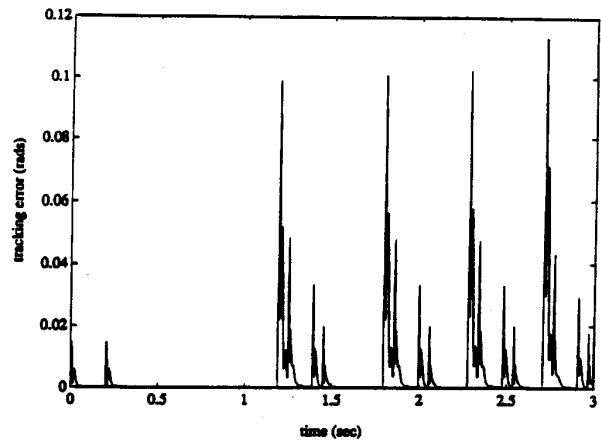


Fig.7. Driving torques of the human-sized biped with local PD control.

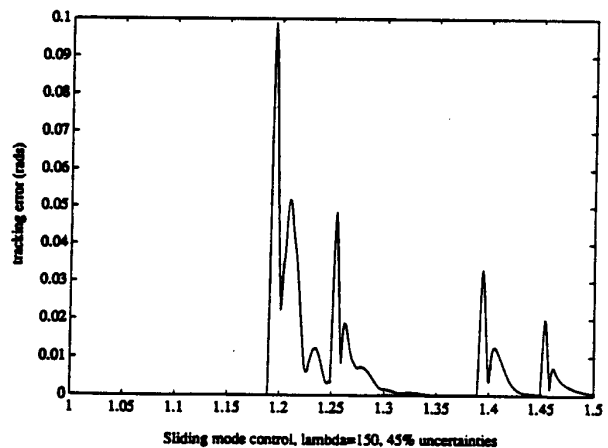
The average tracking error of the computed torque again over a time period of 3 sec is 0.0033 rads (i.e. ten times smaller than that of the local control). However this is achieved through driving torques that are about 10 times larger from the ones corresponding to the small-sized biped of Table 1.

B. Sliding Mode Control

Sliding mode control was applied for several values of the uncertainties $e_m \times 100\%$, $e_l \times 100\%$, $e_1 \times 100\%$ and $e_d \times 100\%$ of the biped parameters m_j , I_j , l_j and d_j . Here we have used the values $e_m = e_l = 0.45$, $e_1 = 0.10$ and $e_d = 0.20$. The results for $\lambda = 150$ and $T_s = 2\text{msec}$ are shown in Figs. 8a and 8b where the variation of the tracking error $|e_1(t)| + |e_2(t)| + |e_3(t)| + |e_4(t)|$ is depicted in an interval of 3sec and around the time of completion of the first step respectively. The average tracking error for the first two steps is 0.0025 rads. One can observe that the error returns to zero despite the existence of parametric uncertainty. The evolution of the angular displacements of the four joints in a period of 3sec is shown in Fig. 9 where



(a)



(b)

Fig.8. Tracking error of sliding mode control with 45% parametric uncertainty and $\lambda=150$.

one can see a very good tracking performance despite the parametric uncertainty.

C. Sliding Mode Versus Computed Torque Control

Here, the results of the sliding mode control will be compared with those obtained via computed torque control. The results obtained using the computed torque control are depicted in Figs. 10 and 11. Comparing Figs. 8 and 10 one observes the considerably increased overshoot and the existence of nonzero steady-state error in the computed torque case. The average tracking error (0.0048 rads) of the computed torque for the first two steps is twice the corresponding error (0.0025 rads) of the sliding mode control. Thus in overall for the same control bandwidth $\lambda=150$ the results obtained through sliding mode control are much better than those obtained via computed torque (smaller overshoot, zero final value of error, much smaller average tracking error).

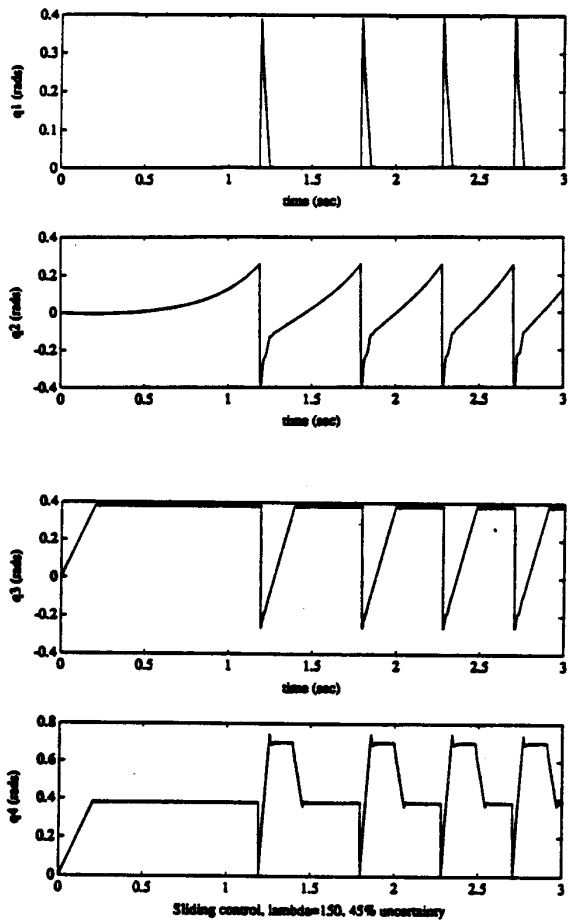
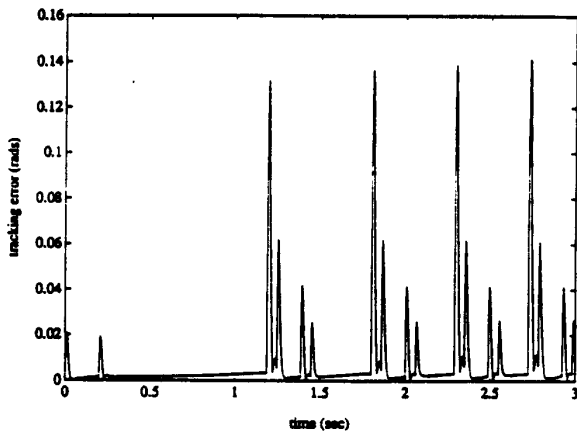
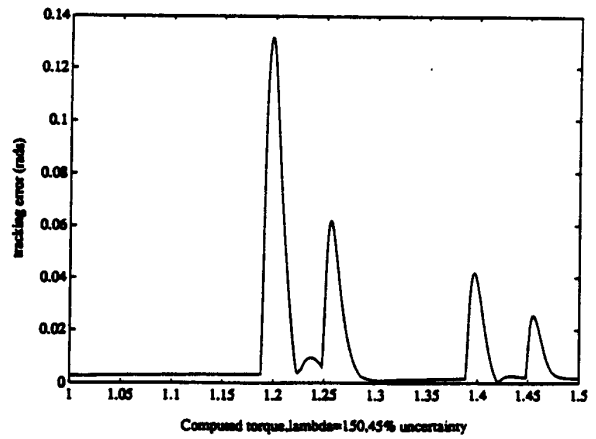


Fig.9. Joint angle trajectories of sliding mode control with $\lambda=150$.



(α)



(β)

Fig.10. Computed torque with $\lambda=150$ under 45% uncertainty.

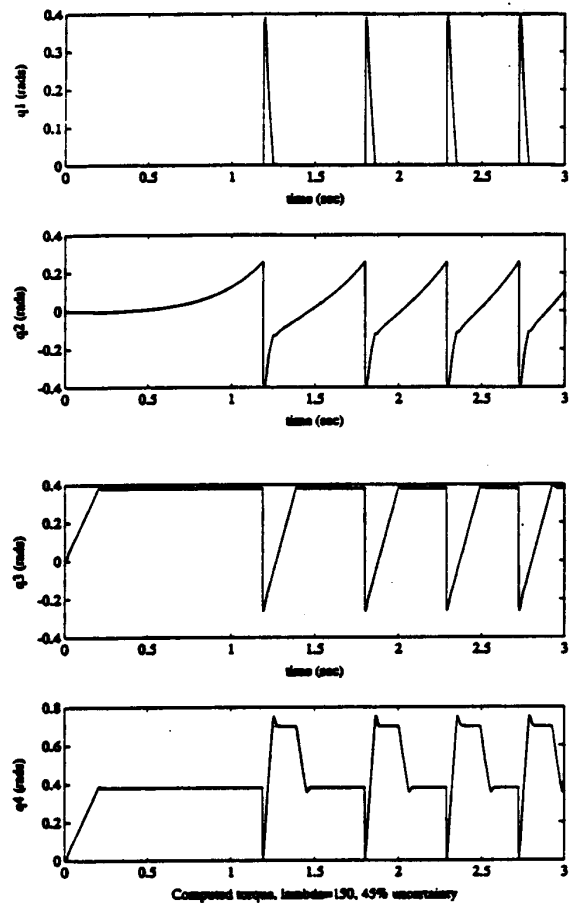


Fig.11. Joint angles during the steady walking on an horizontal plane under computed torque control with $\lambda=150$ and 45% uncertainty.

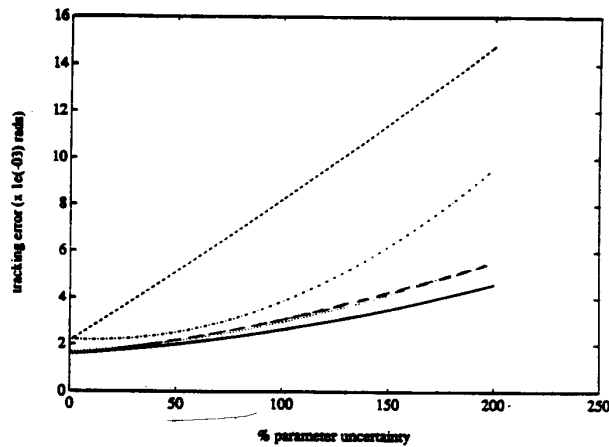


Fig.12. Comparison of the robustness (represented by the average tracking error) of the various control techniques.

The above comparison was made for the parameter uncertainty values $e_m = e_l = 0.45$, $e_1 = 0.10$ and $e_d = 0.20$. However for a full study, this comparison must be made for a sequence of increasing parametric uncertainty. Since the primary source of uncertainty is in the masses and moments of inertia, this study was made by increasing the values of e_m and e_l from 0.10 (10%) to 2.0 (200%) monitoring in each case the average tracking error. The average tracking error obtained over the uncertainty region 10% to 200% is depicted in Fig.12 for the following cases (from top to bottom): computed torque control, sliding mode control with integral term active over the entire boundary layer region, sliding mode control with integral term active over 50% of this region, and sliding mode control with integral term active over 20% of the boundary layer region. The results presented above (as well as others not included here) have fully verified the theoretically expected superiority of the sliding mode control over the computed torque control, especially for situations where there exist large parametric uncertainty.

IV. DIRECTIONS FOR FURTHER WORK

Work is in progress in the following directions:

- to explore biped models with more links (e.g. 9 links or 11 links),
- to explore the performance of alternative robust control schemes [13-15],
- to explore the benefits obtained by using parallel scheduling computational algorithms [16],
- to explore the effectiveness of robust control to handle the situation where one or more robotic arms are attached on the body, considering the effect of their motion as uncertainty to the biped locomotion model.

ACKNOWLEDGEMENT

This work was partially carried out under a visiting exchange grant of the AI Laboratory of MIT. S. Tzafestas expresses his thanks for this opportunity.

REFERENCES

- [1] M. Raibert, "Legged Robots that Balance", MIT Press, Cambridge, Mass., 1986.
- [2] C.K. Chow and Jacobson, "Further studies of human locomotion: Postural stability and control", *Math. Biosci.*, Vol.15, 1972, pp.93-108.
- [3] Hirofumi Miura and Isao Shinoyama, "Dynamic walk of a biped", *Int. J. Robotics Research*, Vol.3, No.2, 1984.
- [4] J. Furusho and M. Masubuchi, "Control of a dynamic biped locomotion system for steady walking", *ASME J. Dyn. Syst. Meas. & Contr.*, Vol.108, 1986, pp.111-118.
- [5] J. Furusho and M. Masubuchi, "A theoretically motivated reduced-order model for the control of dynamic biped locomotion", *ASME J. Dyn. Syst. Meas. & Contr.*, Vol.109, 1987, pp.155-163.
- [6] M. Yamada, J. Furusho and A. Sano, "Dynamic control of walking robot with kick-action", *Proc. 1985 Intl. Conf. on Advanced Robotics (ICAR'85)*, Tokyo, 1985, pp.405-412.
- [7] T. Mita, T. Yamguchi, T. Kashiwase and T. Kawase, "Realization of a high speed biped using modern control theory", *Int. J. Control*, Vol.40, 1984, pp.107-119.
- [8] J.Y.S. Luh, M.W. Walker and R.P.C. Paul, "On-line computational scheme for mechanical manipulators", *ASME J. Dyn. Syst. Meas. & Control*, Vol.102, 1980, pp.69-76.
- [9] Y.F. Zheng and H. Hemami, "Mathematical modeling of a robot collision with its environment", *Int. J. Robotics Research*, Vol.2, No.3, 1985, pp.289-307.
- [10] J.J. Slotine, "The robust control of robot manipulators", *Int. J. Robotics Research*, Vol.4, No.2, 1985.
- [11] J.J. Slotine and W. Li, "Applied Nonlinear Control", Prentice Hall, 1991.
- [12] S. Tzafestas, M. Raibert and C. Tzafestas, "Robust Sliding-Mode Control Applied to a 5-link Biped Robot", (submitted).
- [13] S.G. Tzafestas, L. Dritsas and J. Kanellakopoulos, "Robust robot control: A comparison of three techniques through simulation", In: *Modeling and Simulation of Systems*, (P. Breedverld et al., eds), J.C.Baltzer Co., 1989, pp.255-260.
- [14] S.G. Tzafestas, "Adaptive, robust and rule-based control of robotic manipulators", In: *Intelligent Robotics Systems* (S.G.Tzafestas, Ed.), Marcel Dekker, 1991, pp.313-419.
- [15] I. Jaworska and S. Tzafestas, "Robust stability analysis of robot control systems", *Robotics and Autonomous Systems*, Vol.17, 1991, pp.285-290.
- [16] S.G. Tzafestas, "Task grouping and scheduling for parallel processing", In: *Systems and Control - Topics in Theory and Applications*, (T.Ono and F.Kozin eds.) MITA Press, 1991, pp.401-419.